Crystallography of Stress-Affected Martensite and Bainite

Saurabh Kundu[1], Kazukuni Hase[2], H. K. D. H. Bhadeshia[3]

[1]Tata Steel Limited, Jamshedpur-831001, India, [2] JFE Steel Corporation, Japan, [3] University of Cambridge

The phenomenological theory of martensite crystallography (PTMC) has been developed more than fifty years ago and it helped in answering many questions related martensite and bainitic transformations. Recently researchers are trying to develop models to explain transformation texture under various conditions. It is known that transformation texture is developed in martensite or bainite for applied stress during transformation, which leads to variant selection, or for the presence of prior texture in austenite. However the recent literature shows that there is a trend to avoid the basic crystallographic theory in explaining the texture. In this paper the basic theory is first described and then used to develop models to explain the transformation texture. The theory of variant selection given by Patel and Cohen is also used for the model development. The results obtained are very encouraging.

1. INTRODUCTION

The crystallography of martensite transformation has been a story of exciting scientific development over the years. First, the austenite to martensite transformation has been described with the help of bain strain which is proved to be insufficient to describe the crystallography of transformation and the observed shape change together. Later the phenomenological theory of martensite crystallography (PTMC) has been developed [1, 2] which can explain the experimentally observed shape change as well as the crystallography of transformation together. Martensite transformation is associated with a dilatational strain and a shear strain. The shear strain is much bigger in magnitude (0.22) than the dilatational one (0.03) but the shear stress associated with each martensite variant, which form randomly in the microstructure, cancel each other. However it has been observed that if the martensite is formed under external stress there is a preferred direction along which the plates tend to be aligned. Under this condition the martensite/bainite plates are not randomly oriented but are textured. Recently some work have been published on the prediction of martensite pole figures formed with or without the influence of stress [3–5]. But in most of these studies martensite transformation theory has not been understood properly. In many cases model has been developed considering only the bain strain associated with the transformation, which is insufficient to describe the crystallography of the transformation completely. In some cases the K-S or N-W relationship has been taken as the base to develop the crystallographic relationship between austenite and martensite [5–10], which is not entirely correct. The existence of an invariant line is an essential requirement for martensitic transformation to occur. It is not surprising therefore, that Nolze [11] in his experimental study of several hundred thousand γ/α orientation relations, found detailed deviations from assumed Kurdjumov–Sachs *et al.* orientations.

The present authors have already shown that the transformation texture and variant selection can be explained using suitable mathematical models [12–14] developed following the PTMC theory and the theory outlined by Patel and Cohen [15]. In this paper a detailed analysis of the experimental and simulation results will be presented to understand the effect of external stress on the variant selection, transformation texture and microstructure. The theory and the results presented in this article are applicable to any displacive transformation in general, which includes both martensite and bainite transformation (mentioned as α' in this paper).

2. PHENOMENOLOGICAL THEORY OF MARTENSITE CRYSTALLOGRAPHY

For the α'/γ interface to be glissile, it must as a minimum contain an invariant line. Such a line is one, which is undistorted and unrotated by the invariant-line strain can not be obtained by bain deformation only. Bain deformation simply involves a compression along one of the three axes of FCC austenite crystal and expansion along other two axes.

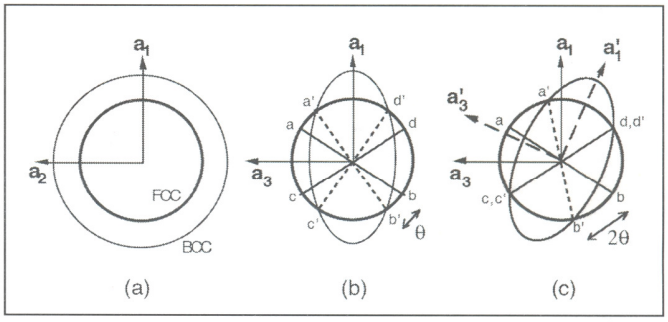

Fig. 1: (a) and (b) represent the effect of the Bain strain on austenite, shown initially as a sphere of diameter ab. On deformation it takes the shape of an ellipsoid. (c) Shows the invariant-line strain obtained by a combined effect of Bain strain and the rigid body rotation [16].

A sphere of austenite is deformed into an ellipsoid by the Bain strain. It can be seen that the lines a' b' and c'd' remain unextended due to the deformation. In fact, the undistorted lines form a right circular cone along a3. However, they are all rotated by an angle θ so they are not invariant. However if a rigid body rotation is now added to the Bain strain, then Fig. 1c illustrates that the rotation makes the initial and final cones of the unextended lines touch along the line c'd'. If the overall deformation is expressed as (F S F) = (F B F)(F J F) which is a combination of the Bain strain and a rigid body rotation, then it leaves a line both unrotated and and undeformed. However this strain is no longer a pure strain as the principal axes are rotated to new positions a'_i.

4. ORIENTATION RELATIONSHIP BETWEEN MARTENSITE AND AUSTENITE

It is important to define the crystallographic relationship (α J γ) between the parent austenite and the martensite. If (γ S γ) is the matrix representing the total transformation strain then it can be shown [16] that:

$$(\alpha \, J \, \gamma)(\gamma \, S \, \gamma) = (\alpha \, C \, \gamma) \quad \text{.....(6)}$$

where (α C γ) is the Bain correspondence matrix. It follows that:

$$(\alpha \, J \, \gamma) = (\alpha \, C \, \gamma)(\gamma \, S \, \gamma)^{-1} \quad \text{.....(7)}$$

(γ S γ) can be determined as shown in [16]. The Bain correspondence matrix can, for example be expressed in the austenite reference frame as:

$$\begin{pmatrix} 1 & \bar{1} & 0 \\ 1 & 1 & 0 \\ 0 & 0 & 1 \end{pmatrix}$$

It is known that in the cubic crystal system there are 24 symmetry elements, each of which can be represented by a matrix. So there are 24 (α J γ) matrices, determined by multiplying (α J γ) with each of the symmetry matrices in turn. Associated with each (α J γ) will be a variant of the habit plane and displacement vectors.

5. DATA

The transformation texture can in principle be calculated from the knowledge of the initial texture of austenite, and by taking into account variant selection due to the applied stress. But in doing so, it is important to realise that the shape deformation, habit plane and orientation relationship of any particular plate of bainite are mathematically connected by the crystallographic theory [1, 21]. A complete set of crystallographic data is therefore necessary before rigourous calculations can be attempted. Unfortunately, such data are frequently not available.

In Table 1 refer to crystallographic data set used to model the bainitic transformation texture in a high carbon steel which has been calculated using methods described in [16]. The lattice

Table 1 : Cryallographic data set for bainite in high C steel.

Habit plane (– 0.168640 – 0.760394 – 0.627185) γ

Shape deformation matrix (γ P γ)

$$\begin{pmatrix} 0.992654 & -0.033124 & -0.027321 \\ 0.026378 & 1.118936 & 0.098100 \\ -0.027321 & -0.123190 & 0.898391 \end{pmatrix}$$

Coordinate transformation matrix (γ Jα)

$$\begin{pmatrix} 0.575191 & 0.542067 & 0.097283 \\ -0.550660 & 0.568276 & 0.089338 \\ -0.008610 & -0.131800 & 0.785302 \end{pmatrix}$$

parameters of interest in the present work, *i.e.*, $\alpha_\alpha = 0.3619$ nm and $\alpha_\alpha = 0.2882$ nm [22]. This results in a macroscopic transformation–strain which is a shear of 0.2292 and a dilatational strain of 0.01 normal to the habit plane. The maximum fraction of bainite possible in the alloy system studied, for a transformation temperature of 300°C, is 0.63 [22].

6. RESULT AND DISCUSSIONS

6.1 Traces of habit plane

It is well known that if α' forms under the influence of stress plates tend to align themselves to a particular angle with the direction in which stress is applied [15]. It is understood that the applied stress helps to form those variants of α' in which the habit planes are aligned favourably so that the energy supplied by the applied stress favours the transformation. If the shear stress associated with the transformation is taken to be 0.2292 and the dilatational component is 0.01 then the angle the habit planes make with the stress axis is about 43.8. [15]. However to model this phenomenon in the two dimensional situation (like what one observes under microscope) it is important to get the traces of the of the habit planes on the plane of observation. The interaction energy between the applied stress and the shear and dilatational strain associated with the transformation has been calculated following equation 4. It is understood that for different variants of martensite value of σ_N and τ would be different because the applied stress makes different angle with normal to the habit plane in each case. The interaction energy is calculated for all variants of α' after finding out the values of σ_N and τ in each case and it is assumed that only the first 3 variants of α' with highest positive interaction energy can form under stress. For calculating the pole figure of the habit planes in a polycrystalline sample an aggregate of 500 grains have been considered. The same calculation is repeated for all the austenite grains present in the microstructure which are randomly oriented and thus the crystallographic orientation relationship between them are assumed to be given by an arbitrary rotation matrix [23]. This way for all the grains predominant variants are selected and the habit planes associated to those variants are plotted in Fig. 3.

When this plot is compared with the pole figure of the martensite habit planes formed without stress (Fig. 4) the difference is apparent. It can be seen that the pole figure under stress is heavily textured whether pole figure without stress is fully random in nature.

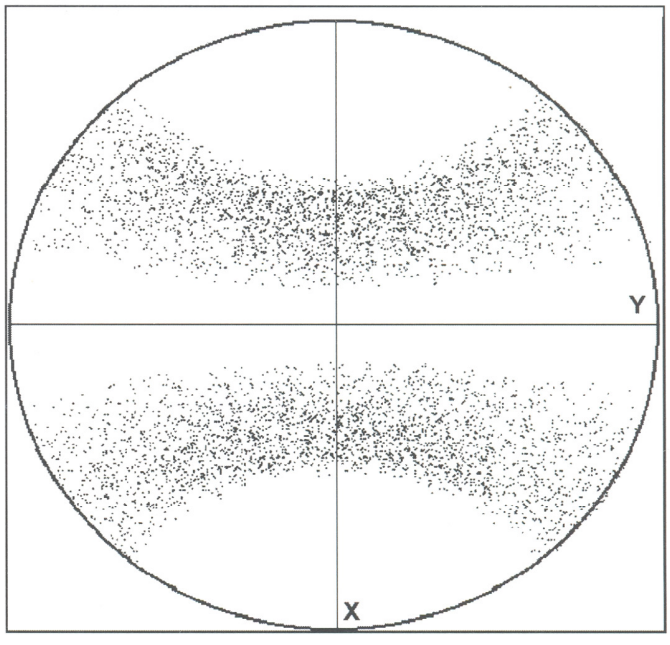

Fig. 3 : Pole figure of habit plane under stress.

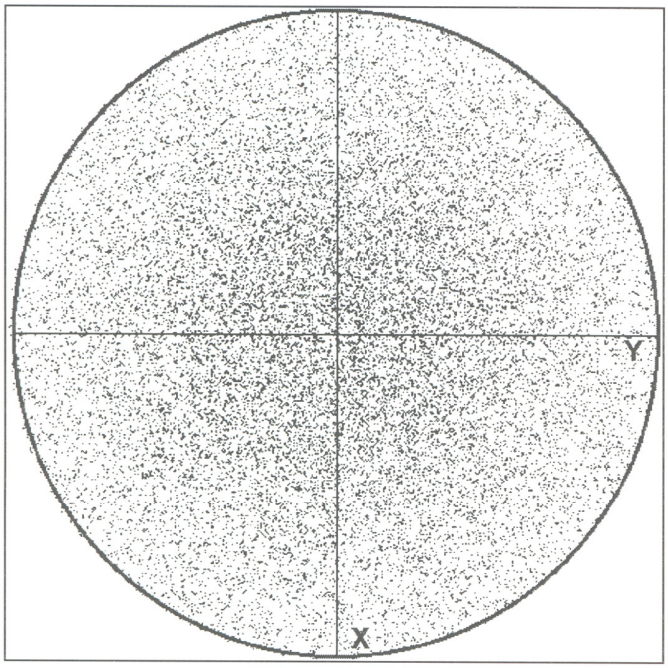

Fig. 4 : Pole figure of habit plane without stress.

This aspect can be shown in a better way by plotting the angle between the trace of habit plane (on the plane of observation) with the direction of applied shear. To find out the angle between the habit plane and the direction of stress first the trace of habit plane on the plane of observation is determined. It can be done by taking the cross product between the unit plane normal of the habit plane with the plane of observation. The resultant vector gives the traces of the habit plane on the plane of observation. The dot product between the traces and the direction of stress gives the angle required. Fig. 5a,b the model predicted distribution of the trace angles associated with various plates of α' which forms under uniaxial tensile stress. In Fig. 5a it is considered that only 2 out of 24 variants are forming (high level of variant selection) and in Fig. 5b weaker variant selection (8 variants forming out of 24) is considered. It is clear from Fig. 5a that in most of the cases the habit plane makes an angle between 40°-50° with the direction of stress when α' forms from austenite under tensile stress with a high degree of variant selection. However under the same condition if the variant selection is less strong (8 variants form) then the distribution of angles made by the traces of the habit plane of the martensite plates with the stress direction is random (Fig. 5b).

It is interesting to note how the distribution of angles changes when martensite or bainite forms from textured austenite. Fig. 6a,b show the distribution of angles with respect to the stress axis when transformation takes place from Goss textured austenite. Fig. 6b shows that even if the variant selection is not very strong and 8 out of total 24 variants are forming most of the plates are aligned at an angle of 60°-70° with the direction of applied stress. There are two important observations to be made from this result. First, most of the martensite/bainite plates are aligned at an angle between 60°-70° with the stress axis when variant selection is less strong, however the angle at which most of the plates are oriented changes to 40°-50° when the variant selection is stronger (Fig. 6a). Secondly the orientation bias remains similar even if the extent of variant selection changes. However for randomly oriented austenite the martensit/bainite plates are biased only when the variantt selection is very strong. These factors will effect the transformation strain and thus the mechanical properties like residual stress in welded joints or elongation in TWIP or TRIP steels will be affected [23].

6.2 Pole figure prediction

Bainite was formed in a high carbon steel under uniaxial compressive load in a thermo–mechanical simulator (*Thermecmaster Z*) following the experimental procedure described in [22]. The specimens were later studied metallographically on their longitudinal sections, and subjected to electron backscattered diffraction (EBSD) in a Hitachi S–4300 and JEOL, JXA6400 scanning electron microscope with a step size of 0.25 μm. A favoured crystallographic variant is one for which the interaction energy with the applied stress is positive, *i.e.*, its macroscopic transformation strain complies with that stress. The purpose here is to demonstrate that favoured variants correspond to the highest observed intensities. Fig. 7 shows the three grains from which EBSD data were collected to produce the pole figures.

Table 2 lists the interaction energies between the bainite variants and the applied stress, with a positive energy denoting a favourable interaction. There are, therefore, 12 to 16 favoured variants in these three grains, within which the first eight are in a class of high values of U with the remainder with much smaller positive interaction energies.

It has already been shown in a previous paper [14] by the present authors that the mathematical models developed follwing PTMC and theory of Patel and Cohen [15] can explain the pole figures obtained from Grain A, B and C (Fig. 7). Additional work has been donc to clarify the plot in Fig. 7. Although it has been argued in [14] that in grain A (Fig. 7) 12 variants are favoured, it is not clear from Fig. 7 that in grain A, there are indeed 12 variants, because the All Euler photograph is not clear on that aspect.

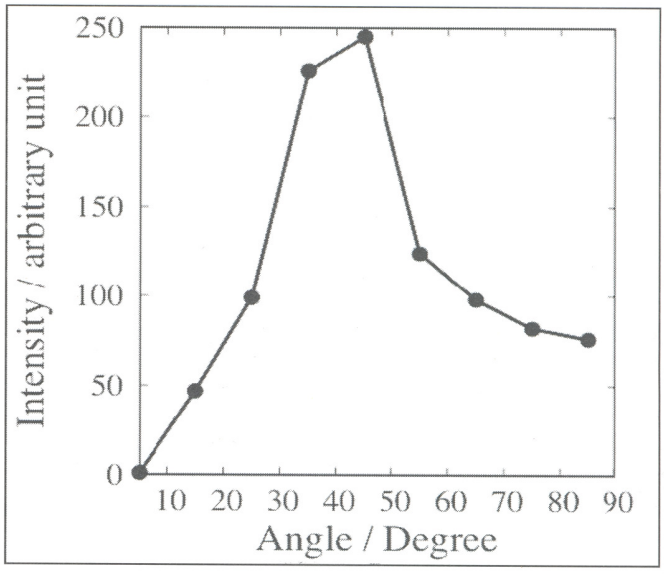

(a)

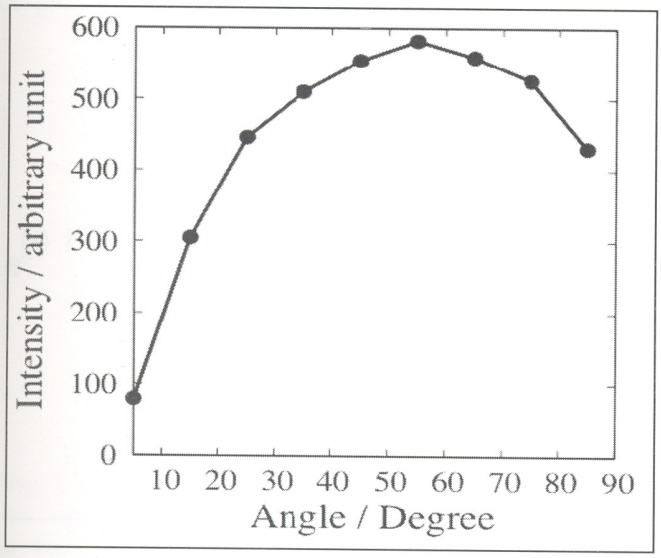

(b)

Fig. 5 : Distribution of angle made by the traces of habit plane of martensite plates formed from austenite under tensile stress with the stress axis. (a) 2 most favourite variants are allowed to form, (b) 8 most favourite variants are allowed to form.

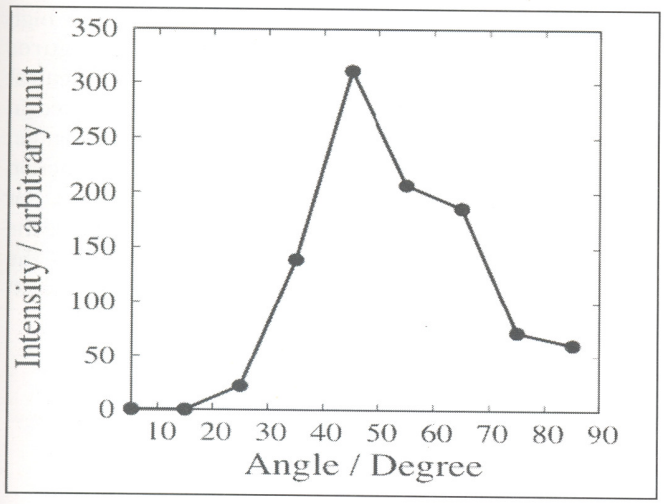

(a)

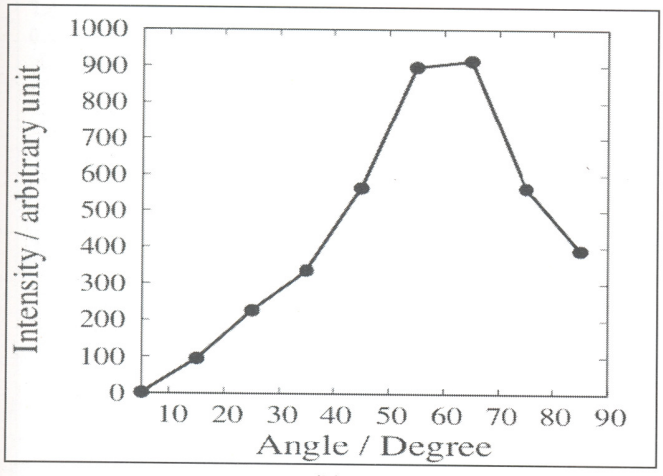

(b)

Fig. 6: Distribution of angle made by the traces of habit plane with the stress axis. (a) 2 most favourite variants are allowed to form, (b) 8 most favourite variants are allowed to form.

Figs 8 and 9 show that it is not possible to explain all the observed intensities without allowing all the twelve favoured variants to form in grain A. Note that in the EBSD analysis presented there, it is not possible to distinguish closely oriented bainite variants. To further analyse the data, the closely oriented variants (8 variants in each group) are clubbed together in groups of similar orientation for the purposes of variant–selection analysis. The interaction energies for all 24 variants in the three grains from Fig. 7 are given in Table 2.

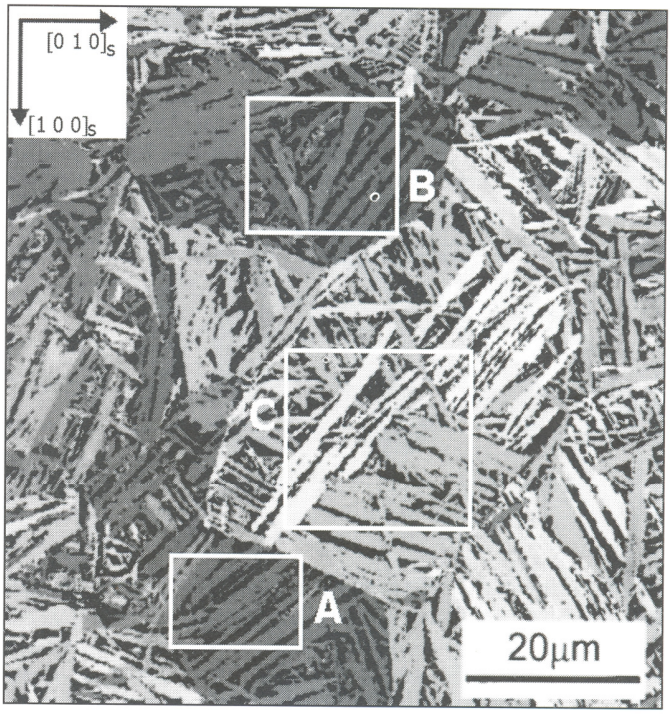

Fig. 7: All Euler image. The colours represent different crystallographic orientations.

Table 2

Interaction energy U (J mol^{-1}) for a uniaxial compressive stress of magnitude 200 MPa, for each of the 24 possible variants of bainite in three grains of austenite. The energies are arranged in descending order, with positive values corresponding to a favourable interaction with the applied stress and *vice versa*. Rank 1 in this listing corresponds to the most favoured variant.

Ranking	1	2	3	4	5	6	7	8
	9	10	11	12	13	14	15	16
	17	18	19	20	21	22	23	24
Grain A	151.2	144.2	133.4	124.6	111.6	111.1	95.7	93.9
	35.6	26.7	24.4	15.7	-7.8	-7.8	-10.9	-12.2
	-126.8	-131.7	-139.0	-145.1	-147.3	-148.8	-152.8	-153.0
Grain B	152.2	151.8	150.4	149.8	143.5	142.9	141.4	141.0
	12.8	12.8	10.9 1	0.7	10.5	10.3	8.4	8.4
	-167.0	-167.3	-168.8	-169.3	-173.9	-174.5	-175.9	-176.3
Grain C	139.6	128.0	95.4	73.1	71.8	65.9	64.6	64.0
	63.2	38.9	4.1	0.9	-4.8	-21.1	-40.0	-40.5
	-64.1	-83.7	-96.1	-98.6	-110.1	-119.3	-119.8	-126.7

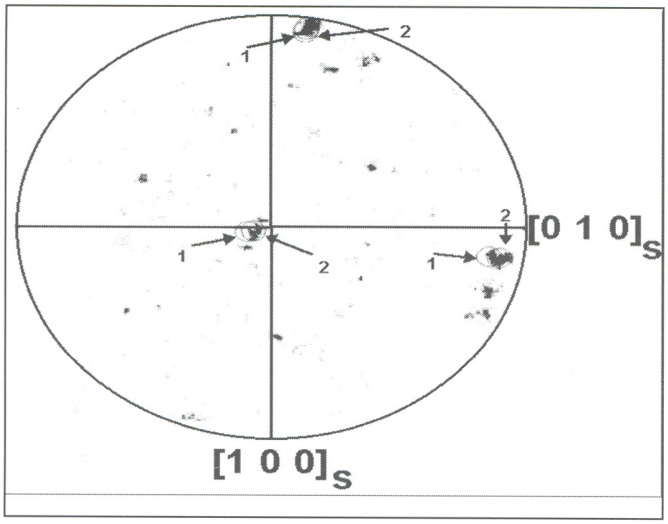

(a)

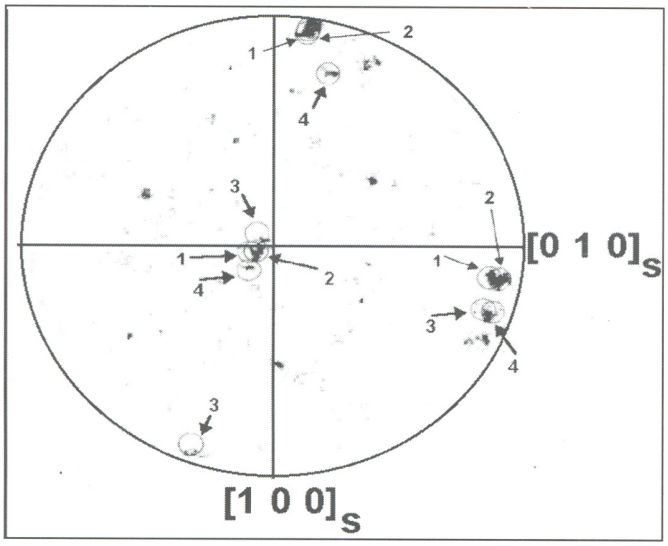

(b)

Fig. 8: $100_{\alpha'}$ pole figure from grain A. Red circles are model predictions. Comparisons with the experimental pole figures is made allowing (a) 2, (b) 4 most–favoured variants to form in the model.

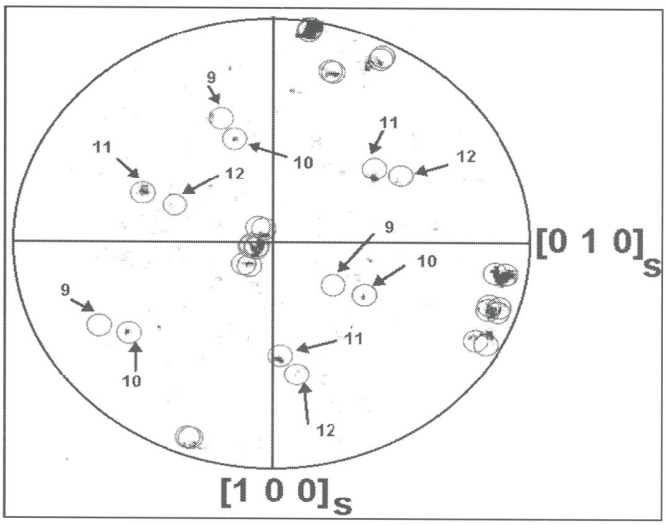

(b)

Fig. 9 : $100_{\alpha'}$ pole figure from grain A. Red circles indicate model predictions. Comparisons with the experimental pole figures is made allowing (a) 8 and (b) 12 most–favoured variants to form in the model.

From Figs 10, 11 and 12, it is evident that the high intensity regions of the experimental pole figures consistently correspond to the variants with the greatest interaction energies. The interaction energies plotted in the bar charts therein represent the summed interaction energy for that cluster of variants. The average interaction energy for each cluster can be deduced from Table 2. For example, in Fig. 10 the average interaction energy for the cluster "X" orientations is 121 J mol-1, which is the average of the interaction energies of the first 8 most favoured orientations listed for grain A in Table 2.

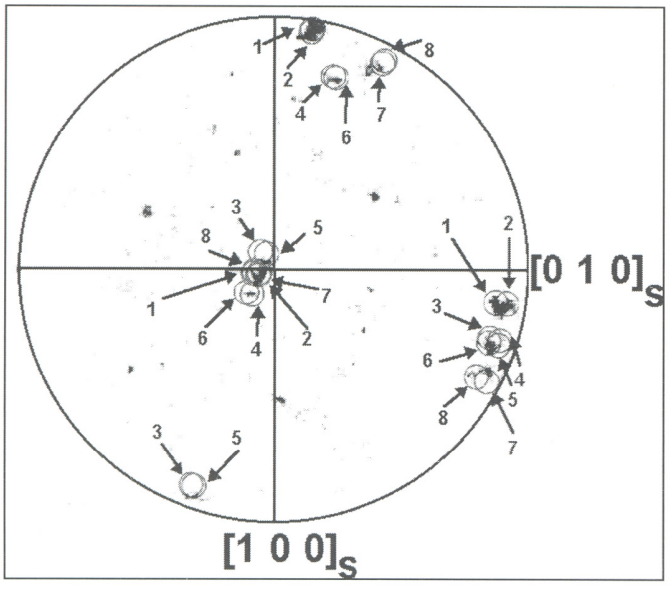

(a)

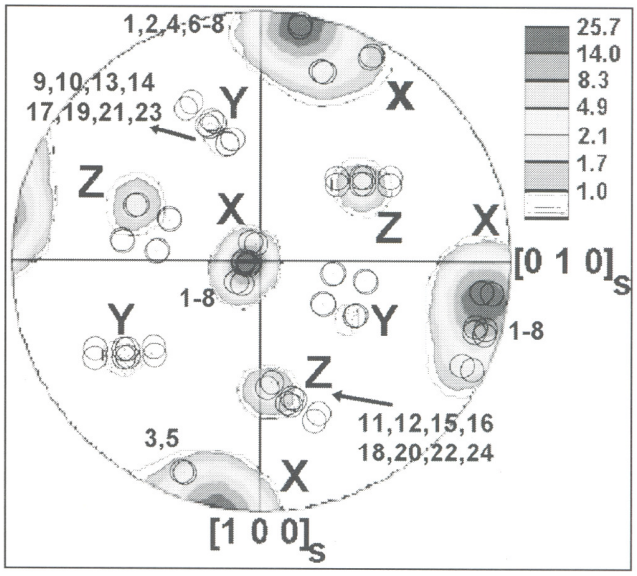

(a)

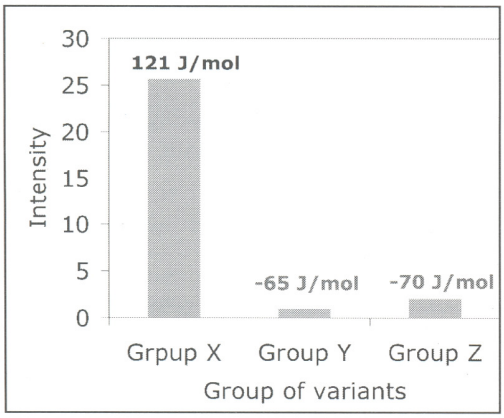

(b)

Fig. 10 : 100$_{\alpha'}$ pole figure from grain A. There are total 24 variants, which includes both favoured and unfavoured variants. (a) The poles are grouped into three regions, X, Y and Z. The numbers indicate variant rankings as listed in Table 2. The colours are indicative of the intensities of poles. (b) Bar chart showing the intensity as a function of region, and the average interaction energy for that region (Table 2).

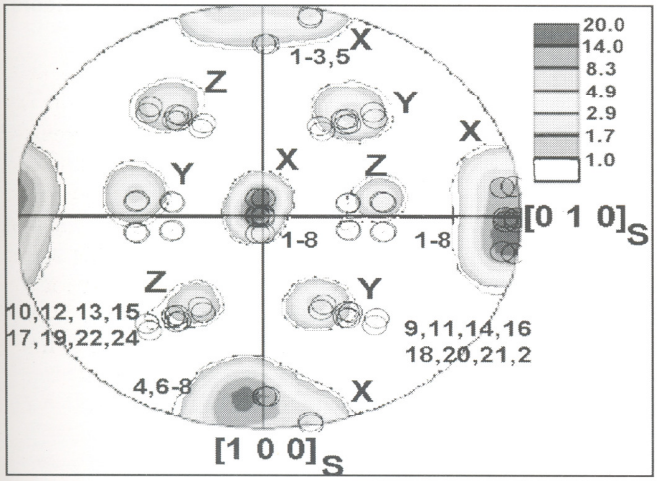

(a)

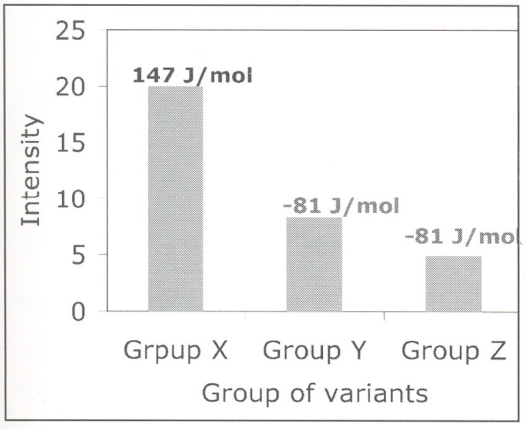

(b)

Fig. 11 : 100$_{\alpha'}$ pole figure from grain B. There are total 24 variants, which includes both favoured and unfavoured variants. (a) The poles are grouped into three regions, X, Y and Z. The numbers indicate variant rankings as listed in Table 2. The colours are indicative of the intensities of poles. (b) Bar chart showing the intensity as a function of region, and the average interaction energy for that region (Table 2).

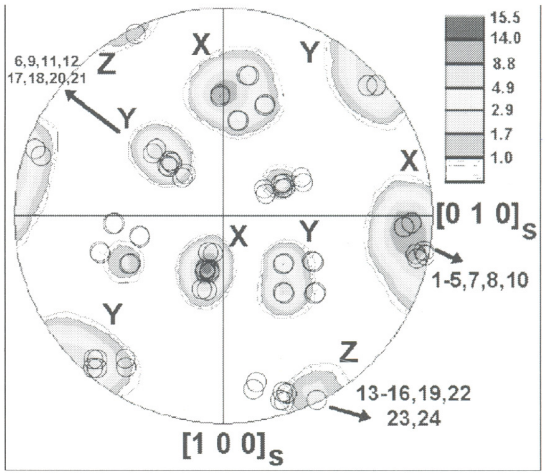

(a)

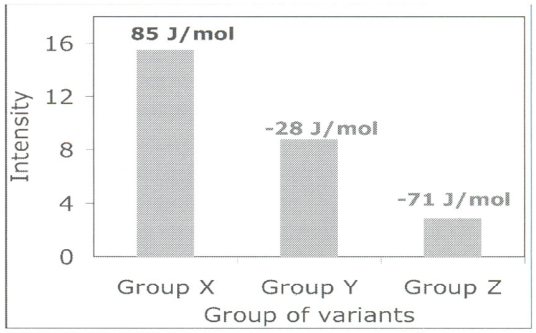

(b)

Fig. 12 : 100$_{\alpha'}$ pole figure from grain C. There are total 24 variants, which includes both favoured and unfavoured variants. (a) The poles are grouped into three regions, X, Y and Z. The numbers indicate variant rankings as listed in Table 2. The colours are indicative of the intensities of poles. (b) Bar chart showing the intensity as a function of region, and the average interaction energy for that region (Table 2).

In summary, whilst it has not been possible to isolate the intensities corresponding to each individual crystallographic variant within a given austenite grain, the work does clearly establish that the largest observed intensities do indeed correspond to the most favoured variants. It must be mentioned here that to model the variant selection the plastic strain theory of Patel and Cohen has been utilised here [15]. Humbert *et al.* has used infinitesimal deformation theory where the transformation strain is treated as elastic [4]. It has already been shown by Kundu and Bhadeshia [13] that, because the strain during martensite transformation is plastic it is always right to use the Patel and Cohen's theory to model variant selection.

7. CONCLUSION

(1) A model has been developed from following the PTMC theory to predict the transformation texture during martensite/marteniste transformation.

(2) The model developed here clearly shows that the Patel and Cohen's plastic strain theory is capable of predicting the variant selection.

(3) It has been shown that there is no need to follow the K-S or N-W type relationships to calculate the texture formation during martensite transformation. The basic limitations of this type of relationships have also been pointed out.

(4) It has been shown that the theory developed in the present work can successfully predict the distribution of angles the habit planes make with the axis of applied stress. It has also been shown that the pole figure of the habit plane of martensite/bainite formed under stress has distinct texture where as the same for martensite/bainite formed without stress shows no distinct texture formation.

(5) Excellent agreement have been observed between the experimental and model predicted pole figures. This shows the strength of model.

REFERENCES

[1] J. S. Bowles and J. K. MacKenzie. *Acta Metallurgica*, 2:129–137, 1954.

[2] J. K. MacKenzie and J. S. Bowles. *Acta Metallurgica*, 2:138–147, 1954.

[3] H. N. Han, C. G. Lee, C.-S. Oh, T.-H. Lee, and S.-J. Kim. *Acta Materialia*, 2004:5203–5214.

[4] M. Humbert, B.Petit, B. Bolle, and N. Gey. *Materials Science and Engineering A*, doi:10.1016/j.msea.2006.11.12, 2007.

[5] P. Bate and B. Hutchinson. *Acta Materialia*, 48:3183–3192, 2000.

[6] S. Godet Y. He and J. J. Jonas. Representation of misorientations in rodrigues–frank space: application to the bain, kurdjumov–sachs, nishiyama–wassermann and pitsch orientation relationships in the gibeon meteorite. *Acta Materialia*, 53:1179–1190, 2005.

[7] N. J. Wittridge, J. J. Jonas, and J. H. Root. A dislocation-based model for variant selection during the γ'- α' transformation. *Metallurgical Transactions A*, 32:889–901, 2001.

[8] L. Kestens, R. Decocker, and R. Petrov. *Materials Science Forum*, 408–412:1173–1178, 2002.

[9] L. Kestens, R. Petrov, and Y. Houbaert. *ISIJ International*, 43:1444–1452, 2003.

[10] B. Br¨uckner and G. Gottstein. *ISIJ International*, 41:468–477, 2001.

[11] G. Nolze. *Zietschrift f¨ur Metallkunde*, 95:744–755, 2004.

[12] S. Kundu and H. K. D. H. Bhadeshia. *Scripta Materialia*, 55:779–781, 2006.

[13] S. Kundu and H. K. D. H. Bhadeshia. *Scripta Materialia*, 57:869–872, 2007.

[14] Saurabh Kundu, Kazukuni Hase, and H. K. D. H. Bhadeshia. *Proceedings of the Royal Society A*, 463:2308–2329, 2007.

[15] J. R. Patel and M. Cohen. Criterion for the action of applied stress in the martensitic transformation. *Acta Metallurgica*, 1:531–538, 1953.

[16] H. K. D. H. Bhadeshia. *Geometry of Crystals*. 2nd edition, Institute of Materials, 2001.

[17] S. P. Timoshenko and J. N. Goodier. *Theory of Elasticity*. McGraw Hill International Book Company, London, 1982.

[18] J. C. Bokros and E. R. Parker. *Acta Metallurgica*, 11:1291–1301, 1963.

[19] T. N. Durlu and J. W. Christian. *Acta Metallurgica*, 27:663–666, 1979.

[20] N. Gey, B. Patit, and M. Humbert. *Metallurgical and Materials Transactions A*, 36:3291–3299, 2005.

[21] M. S. Wechsler, D. S. Lieberman, and T. A. Read. *Trans. AIME Journal of Metals*, 197:1503–1515, 1953.

[22] K. Hase, C. Garcia Mateo, and H. K. D. H. Bhadeshia. *Materials Science and Technology*, 20:1499–1505, 2004.

[23] Saurabh Kundu. *Transformation strain and crystallographic texture in steels*. PhD thesis, University of Cambridge, 2007.